Silicon Nanowires and Silica Nanotubes Seeded by Copper Nanoparticles in an Organic Solvent

Hsing-Yu Tuan,† Ali Ghezelbash, and Brian A. Korgel*

Department of Chemical Engineering, Texas Materials Institute, Center for Nano- and Molecular Science and Technology, The University of Texas at Austin, Austin, Texas 78712-1062

Received November 20, 2007. Revised Manuscript Received January 12, 2008

Crystalline silicon (Si) nanowires were synthesized by adding copper sulfide (CuS) nanocrystals and monophenylsilane (MPS) to supercritical toluene at 500 °C at 10.3 MPa. When a small amount of water and oxygen is added to the reaction, amorphous SiO_2 nanotubes form. In both the nanotube and nanowire reactions, the CuS nanocrystals converted to Cu metal. Because the growth temperature is several hundred degrees below the Cu:Si eutectic temperature at 800 °C, the nanowires and nanotubes both appear to grow by a solid-phase seeding process. Furthermore, a portion of the SiO_2 nanotubes (~5%) were found to be helically coiled. When gold (Au) nanocrystals were added instead of CuS, only SiO_2 nanofibers with solid cores formed and there were no coiled structures. The silica/metal interface morphology was examined for both Cu and Au and found to differ significantly for each metal, which perhaps explains the difference in silica morphology produced by these two metals.

Introduction

Semiconductor nanowires[1] can be made using chemical routes, such as vapor–liquid–solid (VLS),[2,3] solution−liquid–solid (SLS),[4,5] and supercritical fluid−liquid–solid (SFLS)[6–8] methods, and are being explored as active components in new chemical sensors,[9] photovoltaics,[10] electronics,[11,12] medical diagnostics,[13] and optoelectronic[14] devices. Nanotubes[15] are also being explored for these kinds of applications, but their hollow cores make them additionally suitable for use as nanosize containers,[16–18] reaction compartments,[19–22] or nanofluidic pipes to transfer or separate fluids and molecules[15,23,24] in laboratory-on-a-chip applications. Therefore, scalable synthetic routes for nanotubes are desired.

Nanotubes of carbon can obviously be synthesized chemically in relatively high yield. But carbon is unique relative to most materials because its sp^2 bonding gives rise to a sheet-like crystal structure that thermodynamically favors hollow tube formation at high temperatures.[25,26] BN is another example of such a "fullerene-like" material that spontaneously forms tubes at high temperature (i.e., >1000 °C).[27–29] Using metal nanoparticles as catalytic seeds, the nanotube synthesis temperature can be lowered.[30–33] Nanotubes of materials like silica, which do not have sp^2 bonding

* Corresponding author: Tel. (512) 471-5633; fax (512) 471-7060; e-mail korgel@mail.che.utexas.edu.

† Present address: Department of Chemical Engineering, National Tsing-Hua University, Hsinchu, Taiwan 30043, Republic of China.

(1) Korgel, B. A.; Hanrath, T.; Davidson, F. M. In *Encyclopedia of Chemical Processing* **1**; Lee, S. K. B., Ed.; Marcel Dekker: New York, 2006; pp 3191–3203.
(2) Wagner, R. S.; Ellis, W. C. *Appl. Phys. Lett.* **1964**, *4*, 89.
(3) Hu, J. T.; Odom, T. W.; Lieber, C. M. *Acc. Chem. Res.* **1999**, *32*, 435–445.
(4) Trentler, T. J.; Hickman, K. M.; Goel, S. C.; Viano, A. M.; Gibbons, P. C.; Buhro, W. E. *Science* **1995**, *270*, 1791–1794.
(5) Wang, F. D.; Dong, A. G.; Sun, J. W.; Tang, R.; Yu, H.; Buhro, W. E. *Inorg. Chem.* **2006**, *45*, 7511–7521.
(6) Holmes, J. D.; Johnston, K. P.; Doty, R. C.; Korgel, B. A. *Science* **2000**, *287*, 1471–1473.
(7) Hanrath, T.; Korgel, B. A. *Adv. Mater.* **2003**, *15*, 437–440.
(8) Shah, P. S.; Hanrath, T.; Johnston, K. P.; Korgel, B. A. *J. Phys. Chem. B* **2004**, *108*, 9574–9587.
(9) Cui, Y.; Wei, Q.; Park, H.; Lieber, C. M. *Science* **2001**, *293*, 1289–1292.
(10) Law, M.; Greene, L. E.; Johnson, J. C.; Saykally, R.; Yang, P. D. *Nat. Mater.* **2005**, *4*, 455–459.
(11) Cui, Y.; Lieber, C. M. *Science* **2001**, *291*, 851–853.
(12) Duan, X. F.; Niu, C. M.; Sahi, V.; Chen, J.; Parce, J. W.; Empedocles, S.; Goldman, J. L. *Nature* **2003**, *425*, 274–278.
(13) Patolsky, F.; Zheng, G. F.; Lieber, C. M. *Anal. Chem.* **2006**, *78*, 4260–4269.
(14) Huang, Y.; Duan, X. F.; Lieber, C. M. *Small* **2005**, *1*, 142–147.
(15) Goldberger, J.; Fan, R.; Yang, P. *Acc. Chem. Res.* **2006**, *39*, 239–248.
(16) Gasparac, R.; Kohli, P.; Mota, M. O.; Trofin, L.; Martin, C. R. *Nano Lett.* **2004**, *4*, 513–516.
(17) Jayaraman, K.; Okamoto, K.; Son, S. J.; Luckett, C.; Gopalani, A. H.; Lee, S. B.; English, D. S. *J. Am. Chem. Soc.* **2005**, *127*, 17385–17392.
(18) Rossi, M. P.; Ye, H. H.; Gogotsi, Y.; Babu, S.; Ndungu, P.; Bradley, J. C. *Nano Lett.* **2004**, *5*, 989–993.
(19) Halls, M. D.; Schlegel, H. B. *J. Phys. Chem. B* **2002**, *106*, 1921–1925.
(20) Khlobystov, A. N.; Britz, D. A.; Briggs, G. A. D. *Acc. Chem. Res.* **2005**, *38*, 901–909.
(21) Britz, D. A.; Khlobystov, A. N.; Porfyrakis, K.; Ardavan, A.; Briggs, G. A. D. *Chem. Commun.* **2005**, 37–39.
(22) Ogihara, H.; Takenaka, S.; Yamanaka, I.; Tanabe, E.; Genseki, A.; Otsuka, K. *Chem. Mater.* **2006**, *18*, 996–1000.
(23) Mitchell, D. T.; Lee, S. B.; Trofin, L.; Li, N. C.; Nevanen, T. K.; Soderlund, H.; Martin, C. R. *J. Am. Chem. Soc.* **2002**, *124*, 11864–11865.
(24) Lee, S. B.; Mitchell, D. T.; Trofin, L.; Nevanen, T. K.; Soderlund, H.; Martin, C. R. *Science* **2002**, *296*, 2198–2200.
(25) Rao, C. N. R.; Satishkumar, B. C.; Govindaraj, A.; Nath, M. *ChemPhysChem* **2001**, *2*, 78–105.
(26) Tenne, R. *Angew. Chem., Int. Ed.* **2003**, *42*, 5124–5132.
(27) Iijima, S. *Nature* **1991**, *354*, 56–58.
(28) Tenne, R.; Margulis, L.; Genut, M.; Hodes, G. *Nature* **1992**, *360*, 444–446.
(29) Chopra, N. G.; Luyken, R. J.; Cherrey, K.; Crespi, V. H.; Cohen, M. L.; Louie, S. G.; Zettl, A. *Science* **1995**, *269*, 966–967.
(30) Bethune, D. S.; Kiang, C. H.; de Vries, M. S.; Gorman, G.; Savoy, R.; Vazquez, J.; Beyers, R. *Nature* **1993**, *363*, 605–607.
(31) Lourie, O. R.; Jones, C. R.; Bartlett, B. M.; Gibbons, P. C.; Ruoff, R. S.; Buhro, W. E. *Chem. Mater.* **2000**, *12*, 1808–1810.

10.1021/cm703304r CCC: $40.75
Published on Web 02/23/2008

that favors tube formation,[34,35] however, generally require other synthetic approaches; arguably, the most successful chemical approach to date for making nanotubes of these kinds of materials has been through the use of sacrificial templates to generate the tube structure. For instance, the pores of mesoporous substrates can be coated with a material and then the substrate dissolved to leave free-floating nanotubes.[36–41] Sacrificial wire-shaped materials, such as carbon nanotubes and nanofibers,[22,42–44] inorganic nanowires,[45–50] or rod-shaped surfactant aggregates[51–60] have been used as nanotube templates.[61] Reactive templating has also been explored, which is a process in which a nanowire is chemically converted to a hollow nanotube by a surface reaction, as in the conversion of ZnO nanowires to ZnS nanotubes,[62,63] Se nanowires into CdSe nanotubes,[64] and Ag nanowires into Au nanotubes.[65,66] Templating, however, requires multiple synthetic steps—template generation, materials deposition, and template dissolution—and often provides relatively low yields. Direct synthetic routes are more desirable from a manufacturing standpoint, but without sp^2 bonding to induce tube formation, it is challenging to rationally design such systems.

Nonetheless, there is precedent in the literature for direct synthesis of nanotubes of such materials. For example, TiO_2 nanotube "forests" have been produced by direct electrochemical anodization of Ti substrates.[67,68] Amorphous InP nanotubes,[69,70] GaN nanotubes,[71] crystalline AlN nanotubes,[72,73] and Sb_2S_3 nanotubes[74] have been obtained from high temperature vaporization (>1000 °C) and condensation processes; Se,[75] TiO_2,[76,77] ZnO,[78] and perovskite[79] nanotubes have formed under hydrothermal and sonochemical conditions. In these systems, impurities appear to serve as nanotube nucleation and growth sites (i.e., Si for SiO_2; In for InP) for the nanotubes; for example, In,[80] Ge,[81] CdSe,[82] and In_2S_3[83] have promoted amorphous SiO_2 nanotube formation in vapor-phase reactions; a Ni catalyst layer generated GaN nanotubes;[84] Ga metal has induced GaP nanotube formation;[85] Au particles have seeded amorphous Si nanotubes;[86] and CeO_2 particles have promoted TiO_2 nanotube growth under hydrothermal conditions.[87] This evidence shows that a chemical approach to nanotubes (of materials with 3D crystal

(32) Lee, D. C.; Mikulec, F. V.; Korgel, B. A. *J. Am. Chem. Soc.* **2004**, *126*, 4951–4957.
(33) Smith, D. K.; Lee, D. C.; Korgel, B. A. *Chem. Mater.* **2006**, *18*, 3356–3364.
(34) Patzke, G. R.; Krumeich, F.; Nesper, R. *Angew. Chem., Int. Ed.* **2002**, *41*, 2446–2461.
(35) Xiong, Y.; Mayers, B. T.; Xia, Y. *Chem. Commun.* **2005**, 5013–5022.
(36) Martin, C. R. *Science* **1994**, *266*, 1961–1966.
(37) Lakshmi, B. B.; Dorhout, P. K.; Martin, C. R. *Chem. Mater.* **1997**, *9*, 857–862.
(38) Hulteen, J. C.; Jirage, K. B.; Martin, C. R. *J. Am. Chem. Soc.* **1998**, *120*, 6603–6604.
(39) Hoyer, P. *Langmuir* **1996**, *12*, 1411–1413.
(40) Zhang, M.; Bando, Y.; Wada, K.; Kurashima, K. *J. Mater. Sci. Lett.* **1999**, *18*, 1911–1913.
(41) Yen, H.-M.; Jou, S.; Chu, C.-J. *Mater. Sci. Eng., B* **2005**, *122*, 240–245.
(42) Ajayan, P. M.; Stephan, O.; Redlich, Ph.; Colliex, C. *Nature* **1995**, *375*, 564–567.
(43) Satishkumar, B. C.; Govindaraj, A.; Vogl, E. M.; Basumallick, L.; Rao, C. N. R. *J. Mater. Res.* **1997**, *12*, 604–606.
(44) Ogihara, H.; Sadakane, M.; Nodasaka, Y.; Ueda, W. *Chem. Mater.* **2006**, *18*, 4981–4983.
(45) Fan, R.; Wu, Y.; Li, D.; Yue, M.; Majumdar, A.; Yang, P. *J. Am. Chem. Soc.* **2003**, *125*, 5254–5255.
(46) (a) Dong, Z. W.; Zhang, C. F.; Deng, H.; You, G. J.; Qian, S. X. *Mater. Chem. Phys.* **2006**, *99*, 160–163. (b) Nemetschek, V. Th.; Hofmann, U. *Z. Naturforsch.* **1953**, *8b*, 410–412.
(47) Mayya, K. S.; Gittins, D. I.; Dibaj, A. M.; Caruso, F. *Nano Lett.* **2001**, *1*, 727–730.
(48) Zygmunt, J.; Krumeich, F.; Nesper, R. *Adv. Mater.* **2003**, *15*, 1538–1541.
(49) Zhai, T.; Gu, Z.; Dong, Y.; Zhong, H.; Ma, Y.; Fu, H.; Li, Y.; Yao, J. *J. Phys. Chem. C* **2007**, *111*, 11604–11611.
(50) Shen, G.; Bando, Y.; Golberg, D. *J. Phys. Chem. B* **2006**, *110*, 23170–23174.
(51) Jung, J. H.; Lee, S.-H.; Yoo, J. S.; Yoshida, K.; Shimizu, T.; Shinkai, S. *Chem. Eur. J.* **2003**, *9*, 5307–5313.
(52) Jung, J. H.; Shinknai, S.; Shimizu, T. *Chem. Mater.* **2003**, *15*, 2141–2145.
(53) Jung, J. H.; Yoshida, K.; Shimizu, T. *Langmuir* **2002**, *18*, 8724–8727.
(54) Gopalakrishnan, G.; Segura, J.-M.; Stamou, D.; Gaillard, C.; Gjoni, M.; Hovius, R.; Schenk, K. J.; Stadelmann, P. A.; Vogel, H. *Angew. Chem., Int. Ed.* **2005**, *44*, 4957–4960.
(55) Rao, C. N. R.; Govindaraj, A.; Deepak, F. L.; Gunari, N. A.; Nath, M. *Appl. Phys. Lett.* **2001**, *78*, 1853–1855.
(56) Jang, J.; Yoon, H. *Adv. Mater.* **2004**, *16*, 799–802.
(57) Nakamura, H.; Matsui, Y. *J. Am. Chem. Soc.* **1995**, *117*, 2651–2652.
(58) Miyaji, F.; Davis, S. A.; Charmant, J. P. H.; Mann, S. *Chem. Mater.* **1999**, *11*, 3021–3024.
(59) Baral, S.; Schoen, P. *Chem. Mater.* **1993**, *5*, 145–147.
(60) Adachi, M.; Harada, T.; Harada, M. *Langmuir* **1999**, *15*, 7097–7100.
(61) van Bommel, K. J. C.; Friggeri, A.; Shinkai, S. *Angew. Chem., Int. Ed.* **2003**, *42*, 980–999.
(62) Dloczik, L.; Engelhardt, R.; Ernst, K.; Fiechter, S.; Sieber, I.; Könenkamp, R. *Appl. Phys. Lett.* **2001**, *78*, 3687–3689.
(63) Zhang, H.; Yang, D.; Ma, X.; Que, D. *Nanotechnology* **2005**, *16*, 2721–2725.
(64) Jiang, X.; Mayers, B.; Herricks, T.; Xia, Y. *Adv. Mater.* **2003**, *15*, 1740–1743.
(65) Sun, Y.; Xia, Y. *Adv. Mater.* **2004**, *16*, 264–268.
(66) Sun, Y.; Wiley, B.; Li, Z.-Y.; Xia, Y. *J. Am. Chem. Soc.* **2004**, *126*, 9399–9406.
(67) Zwilling, V.; Aucouturier, M.; Darque-Ceretti, E. *Electrochim. Acta* **1999**, *44*, 921.
(68) Macak, J. M.; Tsuchiya, H.; Taveira, L.; Aldabergerova, S.; Schmuki, P. *Angew. Chem., Int. Ed.* **2005**, *44*, 7463–7465.
(69) Bakkers, E. P. A. M.; Verheigen, M. A. *J. Am. Chem. Soc.* **2003**, *125*, 3440–3441.
(70) Yin, L. W.; Bando, Y.; Golberg, D.; Li, M. S. *Appl. Phys. Lett.* **2004**, *85*, 3869–3871.
(71) Yin, L.-W.; Bando, Y.; Li, M.-S.; Golberg, D. *Small* **2005**, *1*, 1094–1099.
(72) Ma, Y. W.; Huo, K. F.; Wu, Q.; Lu, Y. N.; Hu, Y. M.; Hu, Z.; Chen, Y. *J. Mater. Chem.* **2006**, *16*, 2834–2838.
(73) Wu, Q.; Hu, Z.; Wang, X.; Lu, Y.; Chen, X.; Xu, H.; Chen, Y. *J. Am. Chem. Soc.* **2003**, *125*, 10176–10177.
(74) Yang, J.; Liu, Y.-C.; Lin, H.-M.; Chen, C.-C. *Adv. Mater.* **2004**, *16*, 713–716.
(75) Li, X.; Li, Y.; Li, S.; Zhou, W.; Chu, H.; Chen, W.; Li, I. L.; Tang, Z. *Cryst. Growth Des.* **2005**, *5*, 911–916.
(76) Kasuga, T.; Hiramatsu, M.; Hoson, A.; Sekino, T.; Niihara, K. *Langmuir* **1998**, *14*, 3160–3163.
(77) Zhu, Y.; Li, H.; Koltypin, Y.; Hacohen, Y. R.; Gedanken, A. *Chem. Commun.* **2001**, 2616–2617.
(78) Dong, Z. W.; Zhang, C. F.; Deng, H.; You, G. J.; Qian, S. X. *Mater. Chem. Phys.* **2006**, *99*, 160–163.
(79) Mao, Y.; Banerjee, S.; Wong, S. S. *Chem. Commun.* **2003**, 408–409.
(80) Li, Y.; Bando, Y.; Golberg, D. *Adv. Mater.* **2004**, *16*, 37–40.
(81) Hu, J.-Q.; Meng, X.-M.; Jiang, Y.; Lee, C.-S.; Lee, S. T. *Adv. Mater.* **2003**, *15*, 70–73.
(82) Geng, B.; Meng, G.; Zhang, L.; Wang, G.; Peng, X. *Chem. Commun.* **2003**, 2572–2573.
(83) Liang, C.; Shimizu, Y.; Sasaki, T.; Umehara, H.; Koshizaki, N. *J. Mater. Chem.* **2004**, *14*, 248–252.
(84) Li, J. Y.; Chen, X. L.; Qiao, Z. Y.; Cao, Y. G.; Li, H. *J. Mater. Sci. Lett.* **2001**, *20*, 1987–1988.
(85) Wu, Q.; Hu, Z.; Liu, C.; Wang, X.; Chen, Y. *J. Phys. Chem. B* **2005**, *109*, 19719–19722.
(86) Li, C.; Liu, Z.; Gu, C.; Xu, X.; Yang, Y. *Adv. Mater.* **2006**, *18*, 228–234.
(87) Yue, L.; Gao, W.; Zhang, D.; Guo, X.; Ding, W.; Chen, Y. *J. Am. Chem. Soc.* **2006**, *128*, 11042–11043.

structure), analogous to metal seed-particle catalyzed carbon nanotube growth[30–33] or metal particle seeded "VLS" nanowire growth, should be possible.

Here, we report a metal particle-seeded synthesis of amorphous SiO_2 nanotubes, which do not have bonding that favors tube formation. Amorphous SiO_2 nanotubes were produced in supercritical toluene at 500 °C and 10.3 MPa when CuS nanocrystals and monophenylsilane (MPS) were added to the reaction in the presence of small amounts of water and oxygen as oxidizing agents. Without the addition of water and oxygen, crystalline Si nanowires were produced. Transmission electron microscopy (TEM) of the seed particles found at the tips of the nanowires and the nanotubes revealed that the CuS nanocrystals converted to Cu metal during the reactions and that this was in fact the seed material. The CuS seeded reactions are then compared to Au nanocrystal-seeded reactions. Au seeds only produced solid silica nanofibers, instead of tubes. The Au/SiO_2 and Cu/SiO_2 interface morphology is then examined and compared, revealing a qualitative difference between the two materials systems, thus explaining the observed difference in product morphology (i.e., tubes versus fibers).

Experimental Details

Anhydrous toluene (99.8%), anhydrous hexane, and MPS (97%) were purchased from Sigma-Aldrich, stored under nitrogen and used as received. Dodecanethiol-coated gold nanocrystals (5 nm diameter) and oleylamine and octenoic acid-stabilized CuS nanocrystals (12 nm diameter) were synthesized as described previously.[88,89]

Reactor Setup and Procedure. Both Si nanowires and SiO_2 nanotubes were synthesized in a 10 mL Ti grade-2 tubular high-pressure reactor system described previously.[90,91] The reactor is connected to a high-pressure liquid chromatography (HPLC) pump that regulates the reactor pressure and provides a convenient way to inject reactants into the system. The reactor is encased in an insulated brass block, and the reactor temperature is monitored by a thermocouple. The reactor pressure is adjusted by a microcontrol valve attached to the exit port on the reactor. In a nitrogen-filled glovebox (O_2 < 0.2 ppm), a small clean and dried Si wafer is placed in the reactor, which helps to collect the nanowires and nanotubes produced in the reaction. The reactor is sealed in the glovebox and then connected externally to the HPLC pump and placed in the heated brass block. After the reactor reaches the desired temperature (typically ~ 500 °C), anhydrous and oxygen-free toluene is added to the reactor until reaching a pressure of 3.4 MPa.

Silicon Nanowire Synthesis. Once the reactor was preheated as described above, a reactant solution of anhydrous deoxygenated toluene with 150 mM MPS and CuS nanocrystals (at a 150:1 Si/CuS mole ratio) was loaded into a 1 mL syringe in a nitrogen-filled glovebox and then removed from the glovebox and injected into a 500 μL six-way HPLC injection loop (Valco). For Au nanocrystal seeding, the reactant solution was anhydrous deoxygenated toluene with 350 mM MPS and a 1000:1 Si/Au mole ratio. The reactant mixture was added to the reactor at a flow rate of 0.4 mL min^{-1} until reaching a final pressure of 10.3 MPa. After 10 min, the reactor was submerged in an ice water bath for 2 min and then cooled to room temperature by flowing air over it. Most of the nanowire product is collected as a powder on the Si collection wafer in the reactor and on the reactor walls.

Silica Nanotube Synthesis. Silica nanotubes were made using the same procedure as used for Si nanowires, except that water and oxygen were added to the reactant solution by adding "benchtop" toluene to the reactant solutions outside the glovebox before injecting into the reactor. The benchtop toluene was stored in air and was saturated with water and oxygen at their room temperature solubilities of 0.001 vol % and ~1.0 mM, respectively. For all reactions, the total reactant solution volume in the syringe was 1 mL, similar to the Si nanowire reactions, but the amount of benchtop toluene was varied to change the water and oxygen concentrations as desired. For example, to obtain 10 vol % benchtop toluene in the reactant solution, 900 μL of reactant solution was loaded into a 1 mL syringe in the glovebox and then removed from the glovebox, and 100 μL of benchtop toluene was added to the syringe prior to injection into the reactor. The MPS and nanocrystal concentration was the same for all of the reactions.

Materials Characterization. Reaction products were characterized by high-resolution scanning electron microscopy (HRSEM), TEM and scanning transmission electron microscopy (STEM), X-ray energy dispersive spectroscopy (EDS), X-ray diffraction (XRD), and electron energy loss spectroscopy (EELS). HRSEM images were obtained on a LEO 1530 field-emission scanning electron microscope with 1–3 kV accelerating voltage with working distances ranging between 2 to 5 mm, typically by looking at the deposition substrate with the collected product. HRTEM, STEM, EDS, and EELS were performed on a field-emission JEOL 2010F transmission electron microscope equipped with a Gatan parallel-EELS GIFF spectrometer and an Oxford INCA EDS. For TEM and STEM imaging, the nanowires and nanotubes were transferred by scratching the material off the deposition substrate onto a 200-mesh lacey carbon-coated nickel grid (Electron Microscope Sciences). TEM images were obtained at 200 kV accelerating voltage. EELS, line scan EDS, and EDS mapping were performed with the microscope in STEM mode at 200 kV accelerating voltage. EELS spectra were obtained by focusing the electron beam to a 0.7 nm diameter spot and then acquiring spectra as a function of probe position on the nanowire or nanotube. XRD was performed using a Phillips vertical scanning diffractometer using 12°/min scan rate with a 0.02° increment in the continuous locked coupled mode. XRD measurements were performed on nanowires and nanotubes evaporated onto a quartz substrate from concentrated dispersions in chloroform.

Results and Discussion

Silicon Nanowire Synthesis with CuS Nanocrystals. Crystalline Si nanowires form when MPS is thermally decomposed in anhydrous, oxygen-free supercritical toluene at 500 °C and 10.3 MPa in the presence of CuS nanocrystals. Figure 1 shows a scanning electron microscopy (SEM) image of Si nanowires produced in such a reaction, along with high-resolution TEM and XRD data confirming that they are crystalline diamond cubic Si. The reaction yield is comparable to Au nanocrystal-seeded Si nanowire reactions, but the nanowires synthesized in the presence of CuS nanocrystals are slightly shorter, with an average length of 7.4 μm and diameters that range between 5 and 20 nm (as observed by SEM from over 100 wires). (For details about Au nanocrystal-seeded Si nanowires, see refs 90 and 91.) Nanowires were observed with three different growth direc-

(88) Saunders, A. E.; Sigman, M. B., Jr.; Korgel, B. A. *J. Phys. Chem. B* **2004**, *108*, 193–199.
(89) Ghezelbash, A.; Korgel, B. A. *Langmuir* **2005**, *21*, 9451–9456.
(90) Lee, D. C.; Hanrath, T.; Korgel, B. A. *Angew. Chem., Int. Ed.* **2005**, *44*, 3573–3577.
(91) Tuan, H.-Y.; Lee, D. C.; Korgel, B. A. *Angew. Chem, Int. Ed.* **2006**, *45*, 5184–5187.

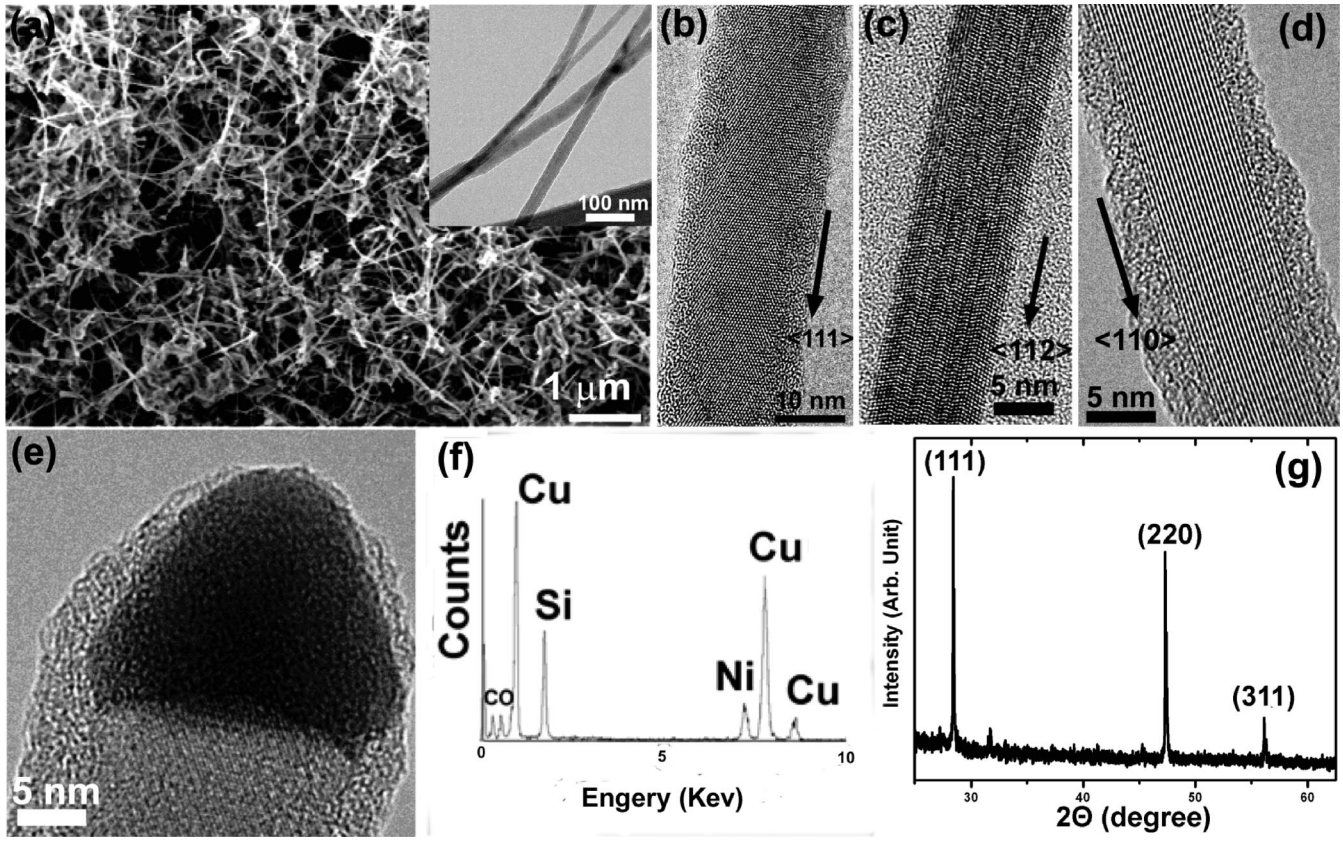

Figure 1. Si nanowires synthesized in supercritical toluene at 10.3 MPa and 500 °C using MPS as a reactant in the presence of CuS nanocrystals. (a) HRSEM image of Si nanowires. Inset: low-resolution TEM of four Si wires. (b−d) TEM images of Si nanowires with three different growth directions: ⟨111⟩, ⟨112⟩, and ⟨110⟩. ⟨111⟩ is the predominant growth direction. (e) TEM image of a Cu−Si alloy particle at the end of a 19.3 nm diameter Si nanowire. (f) Nanobeam EDS data obtained from the metal seed at the tip of a nanowire on a Ni TEM grid, revealing the presence of Cu and Si. (The Ni signal originates from the Ni TEM grid.) (g) XRD peaks from the reaction product match diamond cubic Si (PDF No. 27-1402).

tions, ⟨111⟩, ⟨110⟩, and ⟨112⟩ and Figure 1b−d shows examples of nanowires with each growth direction. Of 104 nanowires examined by high-resolution TEM, ∼75% of the nanowires had grown in the ⟨111⟩ direction, ∼20% in the ⟨110⟩ direction, and ∼5% in the ⟨112⟩ direction. Most of the nanowires observed with a ⟨112⟩ growth direction had lamellar {111} twins running down their length as seen in Figure 1c, which is similar to Si nanowires with λ growth directions produced by SFLS growth with Au nanocrystal seeds.[90,92,93]

Nanobeam EDS (Figure 1f) reveals that Cu and Si are major components of the seed particle, but it is difficult to quantify the Cu/Si ratio due to the background scattering from the Si nanowire. The small C signal might arise from carbonaceous byproducts coating the seed or simply from the background carbon signal of the substrate. The O signal could be from slight oxidation of the copper seed particles after the wire was exposed to air, but as with the C signal, background oxygen adsorbed on the substrate is commonly observed by EDS. Most notably, S is absent from most of tips (>100 tips), indicating that the CuS nanocrystals convert to Cu during nanowire growth. Sulfur was observed in the seed particle of only a few nanowires, but in these cases the nanowires had large diameters and many crystallographic defects (see Supporting Information for details). Kohno and Takeda observed Si nanowire formation from a Si wafer coated with a CuS powder when heated to 1230 °C.[94] Although these reaction temperatures greatly exceed growth temperatures used here (and the nanowire growth mechanism is slightly different, as the wafer was the source of Si for the nanowires), sulfur was also found to diffuse out of the seed particles during the reactions and the nanowires were seeded by copper.

VLS and SFLS nanowire growth requires the formation of a liquid eutectic between the seed metal and the semiconductor at the growth temperature. The nanowire growth temperatures were, however, well below the lowest temperature Cu/Si eutectic at 800 °C.[95] The Si nanowires are therefore most likely growing from solid-phase seed particles. Si has a high solid solubility in Cu, which makes solid-phase nanowire seeding possible, as in the case of Ni and Co seeded Si and Ge nanowires.[96–98] As long as the

(92) Davidson, F. M.; Lee, D. C.; Fanfair, D. D.; Korgel, B. A. *J. Phys. Chem. C* **2007**, *111*, 2929–2935.
(93) Korgel, B. A.; Lee, D. C.; Hanrath, T.; Yacaman, M. J.; Thesen, A.; Matijevic, M.; Kiaas, R.; Kisielowski, C.; Diebold, A. C. *IEEE Trans. Semicond. Manuf.* **2006**, *19*, 391–396.
(94) Kohno, H.; Takeda, S. *Jpn. J. Appl. Phys.* **2002**, *41*, 577–578.
(95) Thaddeus, B. M.; Hiroaki, O.; Subramanian, P. R.; Linda, K.; *Binary Alloy Phase Diagram*, 2nd ed; ASM International: Materials Park, OH, 1990; Vol. 1.
(96) Tuan, H.-Y.; Lee, D. C.; Hanrath, T.; Korgel, B. A. *Nano Lett.* **2005**, *5*, 681–684.
(97) Tuan, H.-Y.; Lee, D. C.; Hanrath, T.; Korgel, B. A. *Chem. Mater.* **2005**, *17*, 5705–5711.

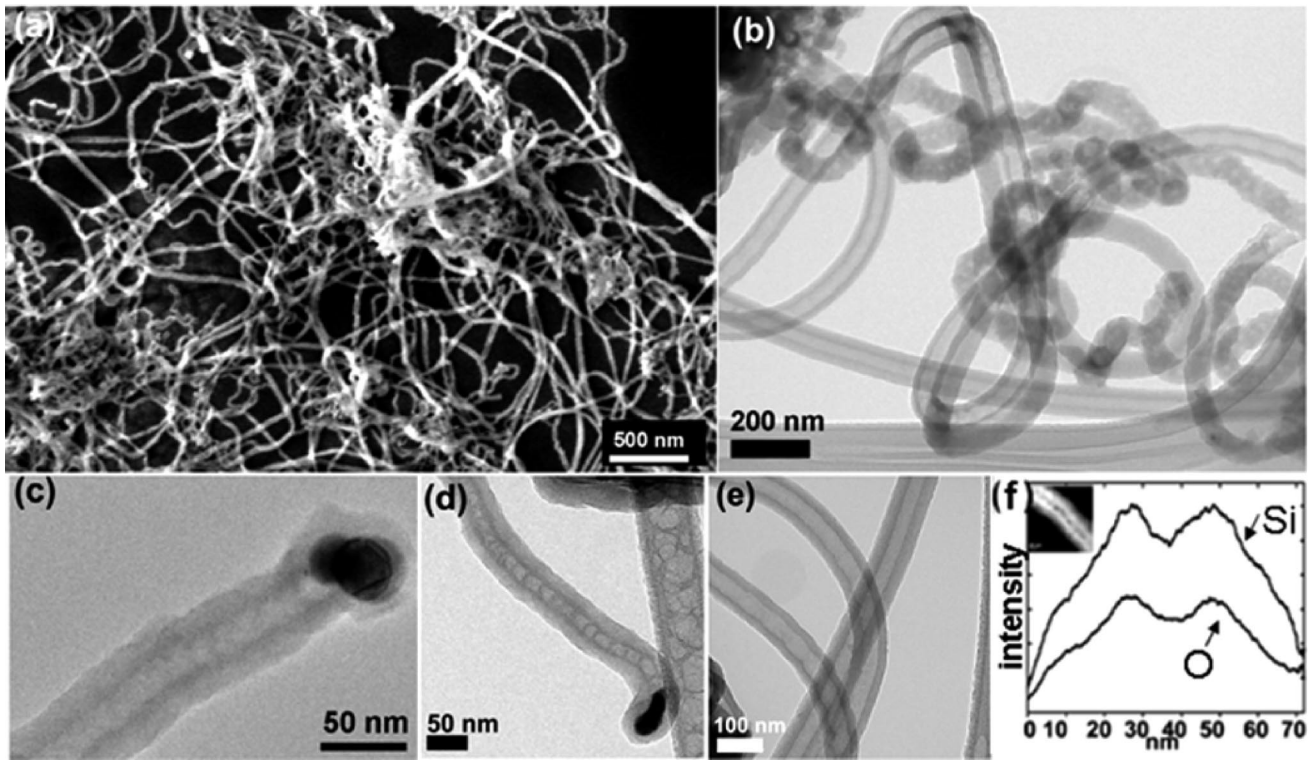

Figure 2. Silica nanotubes produced from MPS with CuS nanocrystals in supercritical toluene at 10.3 MPa at 500° > C with water and oxygen present. The reactant solution injected contained 10 vol % benchtop toluene. (a) HRSEM image of a field of silica nanotubes. (b−e) TEM images of silica nanotubes. The dark particles in the images are Cu. Note that the nanotube in part d has a bamboo morphology. (f) EDS linescans across the silica nanotube in the inset. Both oxygen and silicon are present, and their concentration profiles mirror each other.

seed particles are sufficiently small, solid-state diffusion can maintain nanowire growth (as is the case for the 10−20 nm diameter seeds used here).[97] Yao and Fan[99] also recently demonstrated Cu seeded Si nanowire growth at relatively low temperature, at 500 °C by chemical vapor deposition (CVD) using silane as a reactant.

Silica Nanotube Synthesis. When small quantities of water and oxygen were present in the reaction mixture, MPS decomposition in supercritical toluene at 500 °C and 10.3 MPa in the presence of CuS nanocrystals yielded amorphous silica (SiO_2) nanotubes instead of Si nanowires. Figure 2 shows silica nanotubes produced with a reactant solution containing 10 vol % "benchtop" toluene saturated with oxygen and water, as described in the experimental details. A small number of crystalline Si nanowires were also observed, probably because the water and oxygen concentrations in the reactions were too low to completely oxidize the products (see Supporting Information for details). The SiO_2 nanotubes tended to be shorter and less straight compared to the crystalline Si nanowires synthesized under inert conditions. EDS (Figure 2f) and EELS (Figure 3) both confirmed the nanotube composition to be SiO_2. The Si and O concentration profiles in EDS line scans mirror each other, with both the Si and O signals attenuated when the beam is positioned in the center of the nanotube. In EELS line scans (Figure 3), the absorption edge observed from an Si nanowire (synthesized under inert conditions without water and oxygen) matches the Si L2,3 energy for monocrystalline Si

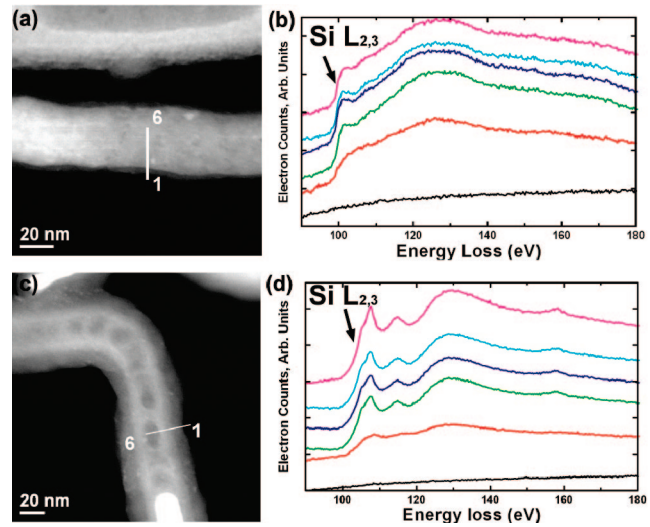

Figure 3. (a, c) STEM images and (b, d) EELS line scans of an (a, b) Si nanowire synthesized in supercritical toluene at 500 °C and 10.3 MPa, CuS nanocrystals under inert conditions with MPS, and (c, d) an SiO_2 nanotube made under similar reaction conditions in the presence of water and oxygen.

at ∼100 eV (Figure 3a,b), whereas the absorption edge observed from SiO_2 nanotubes (synthesized when water and oxygen are present) had a line shape change and energy shift of the Si L2,3 absorption edge to ∼105 eV consistent with SiO_2.[100]

Higher concentrations of "benchtop" toluene (and, thus, water and oxygen) in the reactant solution led to lower yields

(98) Tuan, H.-Y.; Lee, D. C.; Korgel, B. A. *Angew. Chem., Int. Ed.* **2006**, *45*, 5184–5187.
(99) Yao, Y.; Fan, S. *Mater. Lett.* **2007**, *61*, 177–181.
(100) Colder, A.; Huisken, F.; Trave, E.; Ledoux, G.; Guillois, O.; Reynaud, C.; Hofmeister, H.; Pippel, E. *Nanotechnology* **2004**, *15*, L1–L4.

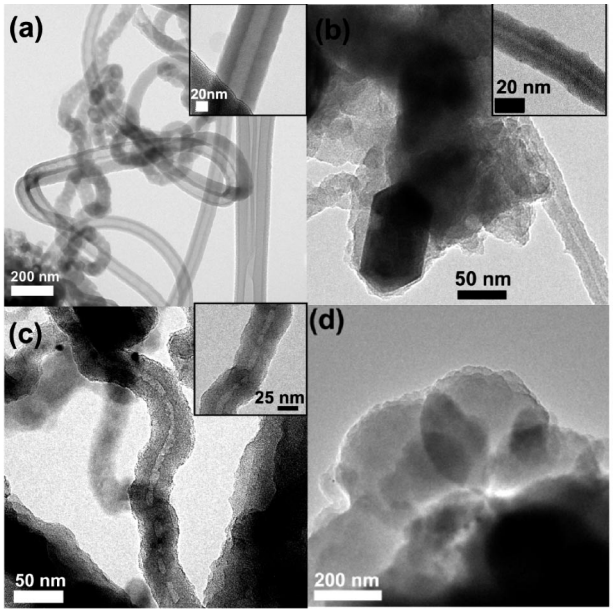

Figure 4. Silica nanotubes synthesized with reactant solutions having increasing amounts of "benchtop" toluene added to the reactant solution: (a) 10 vol %, (b) 25 vol %, (c) 50 vol %, and (d) 100 vol %. (The 100 vol % solution was generated by removing 1 mL of inert reactant solution from the glovebox and allowing it to stand on the bench for 1 h to become saturated with water and oxygen before injection into the reactor).

of silica nanotubes. Figure 4 shows TEM images of the silica nanotubes produced with increasing amounts of "benchtop" toluene added to the reactant solution. The reactions carried out with 10 vol % "benchtop" toluene gave the highest yield of silica nanotubes and the highest quality, with straight and clean silica walls as shown in Figure 4a. Reactions carried out with 25 vol % (Figure 4b) "benchtop" toluene in the reactant solution yielded nanotubes with roughened silica walls and a lower yield of nanotubes and a higher yield of particulates. The 50 vol % "benchtop" toluene in the reactant solutions led to nanotubes with rougher walls (Figure 4c). Only silica particles were produced when 100 vol % "benchtop" toluene was used (see Figure 4d). Although oxygen and water are needed in the reaction to generate SiO_2 instead of crystalline Si, "homogeneous" oxidation of MPS in the bulk of the reactor volume occurs when the oxygen and water concentrations are relatively high, which competes with nanotube formation.

Silica Nanotubes and Nanofibers Seeded with Au Nanocrystals. When Au nanocrystals were used as seeds instead of CuS nanocrystals in the MPS decomposition reactions in toluene at 500 °C at 10.3 MPa with trace water and oxygen in the reactant mixture, a combination of SiO_2 nanofibers and nanotubes (Figure 5) formed, although the majority of the product consisted of solid amorphous SiO_2 nanofibers with only one nanotube for every 20 nanofibers observed. Both the nanofibers and nanotubes made under these conditions were amorphous (by TEM), and EDS confirmed that they were SiO_2.

Helical Silica Nanotubes Seeded by CuS Nanocrystals. Approximately 5% of the SiO_2 nanotubes produced with the injection of CuS nanocrystals were observed to be helically

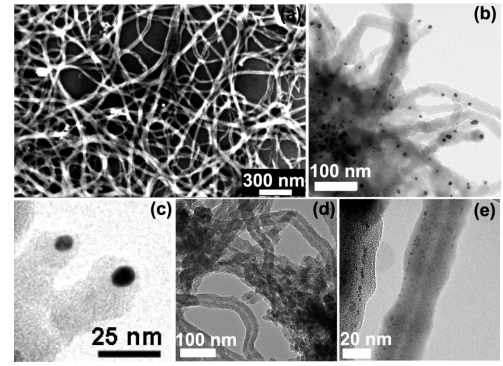

Figure 5. Amorphous silica nanotubes and nanofibers formed with oxygen and water present in the reactant solution, with 350 mM MPS and Au nanocrystals (with Si/Au = 1000:1) in toluene with 10 vol % benchtop toluene in the reactant solution. The reaction was carried out at 10.3 MPa at 500 °C. (a) HRSEM of a field of silica nanofibers; (b, c) TEM images of silica nanofibers with Au nanoparticle at their ends; (d) TEM of a region with a mix of silica nanofibers and nanotubes, and (e) a single silica nanotube. Nanotubes made up approximately 5% of the sample.

coiled like those in Figure 6. Nanotubes were observed to have both right-handed and left-handed helicities, and in some cases, the helicity changed down the length of an individual nanotube, as shown in Figures 6k−m. In some cases, the coiling stopped along the nanotube length. Helical growth has been observed in other chemically grown nanotubes and nanofibers, including Au-seeded silica fibers,[101] metal particle catalyzed carbon nanotubes,[102] Co seeded silica fibers,[103] Fe particle seeded BN fibers,[104] and NiB particle seeded SiC fibers.[105] Amelinckx et al.[102] proposed that the observed helical growth of multiwall carbon nanotubes seeded by metal particles resulted from a variation in the linear growth rate around the circumference of the nanotube at the metal/tube interface that creates a lateral stress that gives rise to coiling. McIlroy and co-workers[101,104,105] proposed that such a variation in growth rate at the metal/seed interface can result from a circumferential difference in contact angle, which they call "contact angle anisotropy", between the metal seed and the nanotube or nanowire. Coiled silica nanotubes were not observed in the Au-seeded reactions, which appears to relate to different wettability or interfacial contact between silica and Au and Cu, as discussed below. Understanding the mechanism that drives coiling in this system requires further study, but the metal/SiO_2 interface appears to be a critical component that can induce coiling under the right conditions.

Silica/Metal Interface Morphology for Au and Cu. To try to understand why CuS nanocrystals yielded predominantly SiO_2 nanotubes, while Au nanocrystals yielded predominantly solid SiO_2 nanofibers (and no coiled structures), reactions were carried out with excess nanocrystals (50:1 nanocrystal/Si molar ratio) and then the interface

(101) Wang, L.; Major, D.; Paga, P.; Zhang, D.; Norton, M. G.; McIlroy, D. N. *Nanotechnology* **2006**, *17*, S298–S303.
(102) Amelinckx, S.; Zhang, X. B.; Bernaerts, D.; Zhang, X. F.; Ivanov, V.; Nagy, J. B. *Science* **1994**, *265*, 635–639.
(103) Qu, Y.; Carter, J. D.; Guo, T. *J. Phys. Chem. B* **2006**, *110*, 8296–8301.
(104) McIlroy, D. N.; Zhang, D.; Kranov, Y.; Norton, M. G. *Appl. Phys. Lett.* **2001**, *79*, 1540–1542.
(105) Zhang, D.; Alkhateeb, A.; Han, H.; Mahmood, H.; McIlroy, D. M.; Norton, M. G. *Nano Lett.* **2003**, *3*, 983–987.

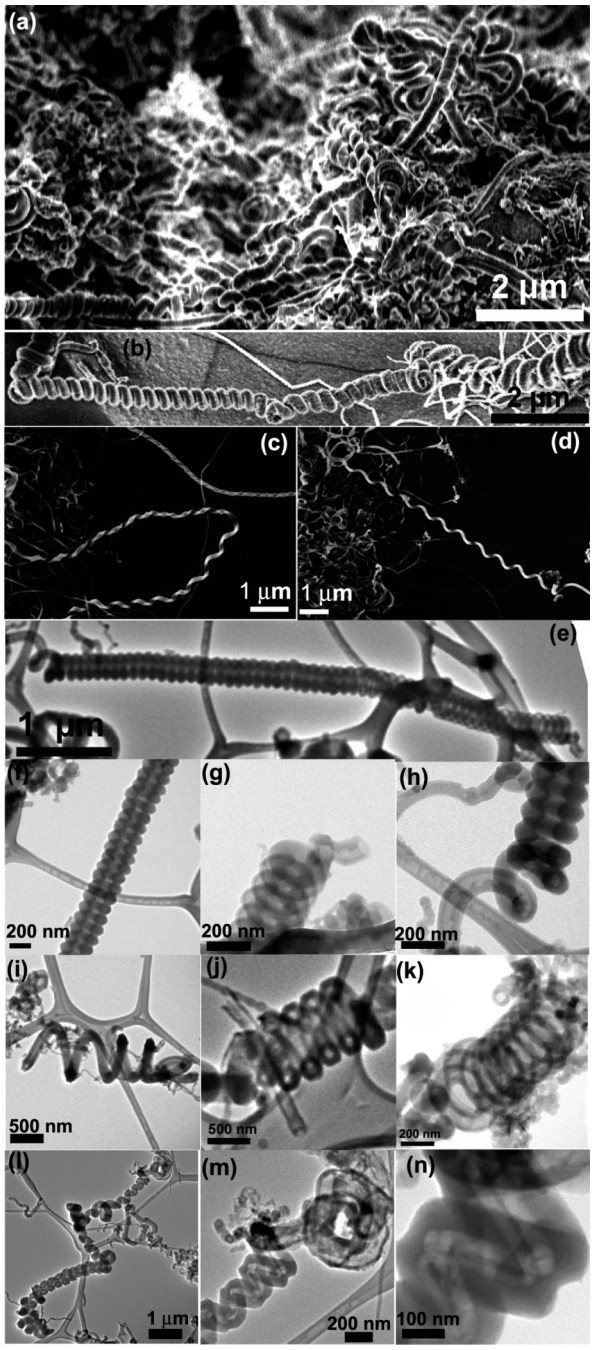

Figure 6. Helical silica nanotubes seeded by CuS nanocrystals in toluene at 10.3 MPa and 500 °C with 150 mM MPS and trace water and oxygen.

structure between the seed metal and the silica produced in the reaction was studied. Only aggregates of silica (or Si under inert conditions) embedded with Cu and Au particles, as shown in Figure 7, were produced at these excessive seed concentrations. There is not a significant difference between Cu/Si and Au/SiO_2 interface morphologies, as the metal particles are approximately spherical and embedded uniformly in the aggregate. In contrast, the Cu/SiO_2 morphology is qualitatively different—the Cu particles have a tear-drop

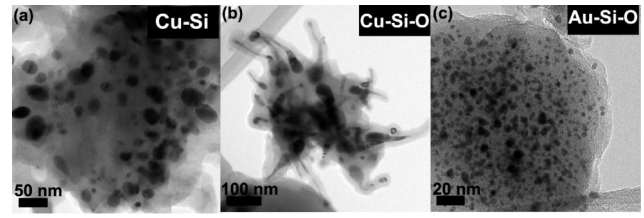

Figure 7. TEM images of (a) Cu nanoparticles embedded in Si formed by MPS decomposition in toluene at 500 °C and 10.3 MPa under inert reaction conditions (i.e., no oxygen and water); (b) Cu nanoparticles embedded in SiO_2 formed when trace oxygen and water were added to the reactions; and (c) Au nanoaprticles embedded in SiO_2 formed when trace oxygen and water were added to the reactions.

shape that is only partially surrounded by silica. A similar "elongated" metal seed particle morphology has also been observed at the tips of multiwall carbon nanotubes synthesized in supercritical toluene at 625 °C[32,33] and was recently reported to be important in in situ growth studies by TEM of metal particle-seeded multiwall carbon nanotubes.[106,107]

Another significant difference between Cu and Au, which may ultimately relate to the difference in silica/metal interface morphology, is that Cu generates Si nanowires by solid-phase seeding,[99] whereas Au forms a liquid eutectic with Si. It is unclear whether a Si nanowire forms, which is subsequently oxidized in the presence of oxygen and water, or if Si oxidizes on the surface of the seed particle and then attaches to the end of the fiber or tube. In the case of Fe particle-seeded growth of multiwall carbon nanotubes, solid carbon fibers were found to form if C dissolved into the seed particle, while nanotubes formed when graphitic carbon appeared to associate only with the nanoparticle surface.[32,108] Silica growth off the surface of the metal seeds is more likely from Cu than Au, since Cu will be present as a solid seed particle, which might favor nanotube formation.

Cu seed particles are also more likely than Au to permit surface oxidation of adsorbed Si. Cu and Au are chemically very different, as Cu can be oxidized easily and could serve as an oxygen sink for oxidizing silicon at the particle surface, while gold is relatively inert to oxidation and is less likely to play a substantial role in Si oxidation. Possibly, the observed difference in Au/SiO_2 and Cu/SiO_2 interface morphology relates to the difference oxidation chemistry that occurs at the metal surface. More experiments are required to fully explore these ideas, but the metal/silica interface morphology is most likely important to the formation of nanotubes.

Conclusions

Crystalline high-aspect-ratio Si nanowires form when CuS nanocrystals are injected with MPS into anhydrous, oxygen-free supercritical toluene at 500 °C and 10.3 MPa. Sulfur diffuses out of the seed particles during the reaction and is not found in the tips of the nanowires; therefore, Cu metal appears to be the active component seeding nanowire growth. The Si nanowires are produced several hundred degrees

(106) Hofmann, S.; Sharma, R.; Ducati, C.; Du, G.; Mattevi, C.; Cepek, C.; Cantoro, M.; Pisana, S.; Parvez, A.; Cervantes-Sodi, F.; Ferrari, A. C.; Dunin-Borkowski, R.; Lizzit, S.; Petaccia, L.; Goldoni, A.; Robertson, J. *Nano Lett.* **2007**, *7*, 602–608.

(107) Lin, M.; Tan, J. P. Y.; Boothroyd, C.; Loh, K. P.; Tok, E. S.; Foo, Y.-L. *Nano Lett.* **2007**, *7*, 2234–2238.

(108) Lee, D. C.; Korgel, B. A. *Mol. Simul.* **2005**, *31*, 637–642.

below the Cu/Si eutectic temperature, evidently by a solid-phase seeding process. When small amounts of oxygen and water are present in the reactions, SiO_2 nanotubes form. Some of these nanotubes (5% of total nanotube product) are helically coiled. When gold nanocrystals are used as seed particles instead of CuS, when water and oxygen are present in the reactant solutions, solid silica nanofibers form with only very few nanotubes. The difference in silica morphology produced by gold and CuS seeds appears to result from qualitative differences between the metal/silica interface morphology for gold and copper. Cu seeds form "tear-drop" shapes, as have been observed for metal seeds involved in the growth of multiwall carbon nanotubes.[32,108] Au seed particles were not observed to take on this shape. Another important difference between Au and Cu is that Cu (unlike Au) readily oxidizes and perhaps enhances MPS oxidation and SiO_2 formation on the metal particle surface, whereas Au serves only as an inert Si sink, leading to an Si nanowire that is then oxidized to SiO_2 as it evolves from the seed particle.

The most significant challenge facing the general design of metal seed particle-directed synthesis of nanotubes is overcoming the tendency of the seed particles to generate solid fibers, as opposed to hollow nanotubes. In "VLS" nanowire growth, crystallization occurs at the metal/semiconductor interface and the nanowire "precipitates" from the seed particle to produce a solid core. Silica nanofibers with solid cores have been produced in several cases from metal seed particles: Chen et al.[109] recently formed SiO_2 nanofibers under hydrothermal conditions using Fe seed particles, Zhang et al.[110] made SiO_2 nanofibers seeded with tin particles, and McIlroy and co-workers[101] made helical silica nanofibers using Au seed particles. In all of these cases the nanofibers were amorphous and the growth process probably was not "VLS" in a strict sense because crystallization would be expected to occur at the metal interface and these structures were not crystalline. This implies that oxidation probably occurred after the nanofiber began to grow. Nonetheless, all of those reactions generated silica fibers with solid cores. In contrast, nanotube formation probably requires silica formation that is in some sense more intimately related to the surface of the seed particle, where a surface adsorbed layer of silica is generated with little diffusion through the volume of the particle and the silica layer wraps around the particle. The interfacial curvature of nanosize seeds would then initiate nanotube formation, much like the folded growth mechanism of carbon nanotubes.[32,33,108]

The study reported here shows that at least in the case of Cu nanoparticle seeding, SiO_2 nanotubes can be generated by a metal nanoparticle-seeding approach. It remains to be determined if the oxidation chemistry of the seed particle is important for nanotube formation or if it is simply a matter of the interfacial energies between the silica and the metal that directs nanotube formation. It appears that metal nanoparticle seeding could be exploited as a general route to the formation of metal oxide nanotubes.

Acknowledgment. This work was supported by the National Science Foundation through their NIRT (DMR-0210383) and STC programs, the Robert A. Welch Foundation, the Advanced Materials Research Center in collaboration with International SEMATECH, the Advanced Processing and Prototype Center (AP2C: DARPA NR0011-06-1-0005), and the Office of Naval Research (N00014-05-1-0857). We also thank J.P. Zhou for TEM assistance.

Supporting Information Available: TEM images of seed particles observed at the tips of some Si nanowires with sulfur. TEM images of crystalline Si nanowires observed in reactions with trace oxygen and water. This material is available free of charge via the Internet at http://pubs.acs.org.

CM703304R

(109) Chen, P.; Xie, S.; Ren, N.; Zhang, Y.; Dong, A.; Chen, Y.; Tang, Y. *J. Am. Chem. Soc.* **2006**, *128*, 1470–1471.
(110) Zhang, J.; Xu, B.; Yang, Y.; Jiang, F.; Li, J.; Wang, X.; Wang, S. *J. Non-Cryst. Solids* **2006**, *352*, 2859–2862.